View metadata, citation and similar papers at core.ac.uk

brought to you by CORE

provided by CiteSeerX

Journal of Membrane Science and Research 1 (2015) 26-33

Journal of Membrane Science and Research

homepage: www.msrjournal.com

Research Paper

Investigation and characterization of TiO_2-TFC nanocomposite membranes; membrane preparation and UV studies

Y. Mansourpanah*, E. Momeni Habili

Membrane Research Laboratory, Lorestan University, Khorramabad, Iran

HIGHLIGHTS

- Different aspects of modification of polyamide TFC membranes by TiO_2 nanoparticles
- Comparing the presence or absence of UV irradiation during the process

ARTICLE INFO

Article history:
Received: 2014-05-27
Revised: 2014-07-28
Accepted: 2014-08-12

Keywords:
Thin film composite
Modification
TiO_2 nanoparticles
MWCO

ABSTRACT

The purpose of this study was to compare the presence or absence of UV irradiation on the separation performance and morphology of the TiO_2-assembled thin film membranes (in different concentrations). Furthermore, an attempt was made to show and compare the effect of the presence of TiO_2 nanoparticles in aqueous and organic phases during the interfacial polymerization process. SEM, zeta potential, water contact angle, and other characterization methods like the molecular weight cut-off (MWCO), as well as antifouling measurements and the separation ability tests were utilized to characterize the thin layer properties. SEM images showed an integrated distribution of the nanoparticles under the PA skin layers. The rejection capability against the sugars was increased with the growth of TiO_2 concentration in the absence of UV. Accordingly, the MWCO of the membranes changed from 420 Da to less than 150 Da. In this case, the flux recovery ratio significantly enhanced while the surface negative charge increased. On the other hand, the membrane pore sizes increased under UV irradiation. Changes in flux and separation performance were significant and considerable during the lack of UV irradiation in comparison with using UV.

© 2014 MPRL. All rights reserved.

1. Introduction

Most commercial membranes have a thin-film composite (TFC) structure [1-4]. A composite membrane is fabricated by forming an ultra-thin dense layer on a porous support layer. In a TFC membrane, each layer can be optimized for its particular function. In this kind of membrane, there are at least two layers in which the support layer provides the appropriate mechanical power with low resistance to permeate flow and the top layer can be designed and optimized for better performance, e.g. desirable permeate flux and rejection. In the literature there are several processes to prepare the TFC membranes; interfacial polymerization being one of the most commonly used processes. For the first time, P.W. Morgan explained and described the interfacial polymerization in detail in 1965 [5]. Accordingly, the polymerization reaction takes place at the interface of the two liquids which are insoluble to each other. Different methods of membrane preparation and modification may be used to improve the separation performance, such as surface modification, blending, copolymerization, adding nanoparticles, and grafting of a selective species onto an inert film [6-10].

Using different inorganic compounds in the structure of polymeric membranes is gaining grow up to improve the properties of the membranes. These membranes, which were commonly called mixed-matrix membranes (MMMs), show good properties. The presence of these particles strongly changes the properties of the polymeric membranes. Their structure consists of an inorganic material incorporated into a polymeric matrix. In fact, the incorporation of the inorganic component can be seen as a relatively easy modification of existing methods for manufacturing large-surface area polymeric membranes; therefore, MMMs possess an economic advantage over inorganic membranes. In addition, they may offer enhanced physical, thermal, and mechanical properties for aggressive environments and could be a way to stabilize the polymer membrane against easy changes.

However, there are many researches which have focused on the use of TiO_2 nanoparticles as a catalytic modifier either in membrane bulk or membrane surface for changing the morphology and performance due to its photocatalytic and super-hydrophilicity effects [11-16]. According to the results, the presence of TiO_2 nanoparticles in the structure of the prepared membranes obviously showed remarkable changes in the membrane performance, especially antifouling properties. This phenomenon helps to solve the membrane fouling problems. Approximately, UV irradiation was utilized in all of the works. The question was how the lack of UV can affect

* Corresponding author at: Tel: +98 66 33120611; Fax: +98 66 33120618.
E-mail address: mansourpanah.y@lu.ac.ir and jmansourpanah@yahoo.com (Y. Mansourpanah).

and change the membrane characteristics.

In this work, an attempt is made to compare the presence or absence of UV irradiation and show its different effects on the membrane separation performance and morphology. Assembling the small amounts of TiO_2 nanoparticles in the structure of poly(piperazineamide) thin layers during the interfacial polymerization was studied, especially the effect of the presence of TiO_2 nanoparticles in the organic and aqueous phases, separately. SEM, zeta potential, water contact angle, molecular weight cut-off (MWCO) test, antifouling properties, and separation ability measurements were utilized to determine the thin layer characteristics.

2. Experimental

2.1. Materials

Polyethersulfone (PES Ultrason E6020P with MW=58,000 g/mol) in powder form was purchased from BASF (Germany) for the formation of porous supports. *N,N*-dimethylformamide (DMF), trimesoyl chloride (TMC), ribose (monosaccharide, MW=150.3 gr/mol), sucrose (disaccharide, MW=342.3 gr/mol) and raffinose (trisaccharide, MW=504.5 gr/mol) were purchased from Sigma-Aldrich (Milwaukee, USA). Poly(vinyl pyrrolidinone) (PVP) with 25,000 g/mol molecular weight, piperazine (PIP) and triethylamine (TEA) from Merck were used. Bovine Serum Albumin powder [some properties are followed: assay; >96%, mol wt.; 66 kDa, pH≈7, solubility >40mg/mL in H_2O] was obtained from Sigma. TiO_2 nanoparticles (TiO_2, particle size of 10 nm) were purchased from US Research Nanomaterials, Inc. Distilled water was also used throughout the study.

2.2. Preparation of PES support

The polyethersulfone support was prepared by dissolving 18 wt.% of PES in dimethylformamide (DMF) with 10 wt.% polyvinylpyrrolidone (PVP) by stirring for 4 h at 50 °C. The stirring was carried out at 300 rpm. After formation of a homogeneous solution, the dope solution was held at the ambient temperature for around 4 h to remove the air bubbles. Afterwards, the dope solution was casted on a non-woven polyester (150 µm thickness) with 75 µm thickness using a film applicator at room temperature. After casting it was immersed into a distilled water bath for at least 24 h for removing most of the solvent and water-soluble polymer.

2.3. Fabrication of TiO_2 embedded-thin film composite membranes

The neat thin layer membranes were prepared through the polymerization of aqueous PIP and organic TMC solutions. The procedure of the formation of the PA thin-film-composite (TFC) membrane has been explained elsewhere [17]. Briefly, the aqueous phase containing PIP (0.15 wt.%) and TEA (0.4 wt.%) was poured onto the support. Then, the trimesoyl chloride solution (0.1 wt. % in hexane) was poured onto the support, in order for the conventional interfacial polymerization reaction to occur. Consequently, a thin layer of PA was formed on the support membrane.

The effect of different concentrations of TiO_2 nanoparticles was investigated in two ways: i) *the presence of TiO_2 nanoparticles in the aqueous phase*: an aqueous phase containing PIP, TEA and different concentrations of TiO_2 nanoparticles (0.005%, 0.01%, and 0.03 wt.%) (which was sonicated before usage) was poured onto the support. Then, the support and aqueous solution were immediately exposed to UV irradiation for 120s in 160 W power. After draining off the excess solution, the organic solution composed of trimesoyl chloride was poured onto the support. ii) *the presence of TiO_2 nanoparticles in the organic phase*: after pouring the aqueous solution on the support and draining off the excess amount, the organic solution composed of trimesoyl chloride and different concentrations (0.005%, 0.01%, and 0.03 wt. %) of TiO_2 nanoparticles (which was sonicated before usage) was poured onto the support and the organic phase was exposed to UV irradiation for 120s in 160 W powers. All of the modified membranes were prepared both with and without using UV irradiation at ambient temperature.

2.4. Permeability and fouling quantification

The flux and rejection of each membrane were determined at 10 min intervals under 0.8 MPa in a dead-end filtration cell. The experiments were carried out at 25 oC. The permeation rate and salt rejection were determined for all membranes using the Na2SO4 solution of 1000 ppm concentration. The molecular weight cut-off (MWCO) of the membranes was determined by the rejection performance of ribose, sucrose and raffinose sugars. The rejection was calculated by using the following equations (1 and 2):

$$R\%_{salt} = \left[1 - \frac{\lambda_p}{\lambda_f}\right] \times 100 \quad (1)$$

$$R\%_{sugar} = \left[1 - \frac{c_p}{c_f}\right] \times 100 \quad (2)$$

Where λ_p, λ_f, c_p and c_f referred to the ion conductivity and the sugar concentrations in the permeate and feed solutions, respectively.

Fouling can be calculated and verified by detecting the resistance appearing during the filtration, and cleaning can be determined by removing this resistance. The resistance can be related to the formation of a cake or gel layer on the membrane surface during the filtration process. Permeate samples were collected over a given period and weighed. The flux (J) through the cake and the membrane may be described by Equation 3:

$$J = \frac{m}{A\Delta t} \quad (3)$$

Where m is the mass of permeated water, A is the membrane area and Δt is the permeation time. Initially the pure water permeate flux was measured and this value was used as a reference for the membrane permeability (J_{wi}). Subsequently, in order to investigate the fouling, the solution reservoir was refilled with a 0.3 g/L BSA solution and the flux was obtained (J_p). The BSA solution was stirred at a rate of 300 rpm. After 2 h of filtration, the membrane was washed with deionized water for 10 min and the water flux of the cleaned membranes was measured (J_{wc}). In order to assess the fouling-resistance capability of the membrane, the flux recovery ratio (FRR) was calculated using Equation 4:

$$FRR = \left(\frac{J_{wc}}{J_{wi}}\right) \times 100 \quad (4)$$

2.5. Membrane characterizations

The SEM microscope (KYKY model-EM3200) was employed to investigate the membrane morphology. The membrane samples were frozen in liquid nitrogen and fractured to the pieces with 1 cm^2. Afterward, they were sputtered with gold and viewed at 25 kV.

The static contact angles were measured with a contact angle measuring instrument (G10, KRUSS, Germany). Deionized water was used as the probe liquid in all measurements and the contact angles between water and the membrane surface were measured for the evaluation of the membrane hydrophobicity. To minimize the experimental error, the contact angle was measured at five random locations for each sample.

The zeta potential was determined by streaming potential measurements for assessment of the charge of the membrane surface. The zeta potential of flat surfaces can be measured by either the streaming potential or electro-osmosis method. The streaming potential method is preferred over electro-osmosis when measuring the zeta potential of flat surfaces. It is more convenient to measure small electrical potentials rather than small rates of liquid flow. In these measurements, a streaming potential is induced when ions within an electrical double layer are forced to move along with a flow, thereby generating a potential difference. Zeta potentials of the prepared membranes were measured by an Electro Kinetic Analyzer (EKA 1.00, Anton-Paar, Swiss) equipped with a plated sample cell. The membrane samples were rinsed thoroughly and soaked in de-ionized water for 2 h and then cut in 2 cm×2 cm size plates. The measurements were carried out at 25 °C in 0.001 M KCl solution with poly(methyl methacrylate) (PMMA) as the reference plate (dimension of reference plate was about 50 mm×38 mm×10 mm). The zeta potential was measured 4 times, and the average value was reported.

The performance of the prepared membranes was analyzed using the dead-end system including a 100 ml stirred filtration cell. The membrane surface area in the filtration cell was 12.56 cm^2. The required pressure was supplied by a nitrogen gas cylinder. The permeate was collected and weighted during the experiments by an analytical balance. The ion rejection was investigated by measuring the permeate conductivity using a conductivity meter (Hanna 8733 Model, Italy). The MWCO of the thin layers was obtained by measuring the sugar concentrations in the feed and permeate using UV-Vis spectrometry (Shimadzu, Japan) [18,19]. Generally, filtration of uncharged solutes at low concentrations is used to determine the MWCO of membranes. The MWCO test is a procedure to determine the nominal pore size of the membranes. Membrane performances are compared by their MWCO, which was usually defined as the smallest molecular weight species for which the

membrane has more than 90% rejection.

3. Results and discussion

3.1. Effect of the presence of TiO_2 nanoparticles in the aqueous phase

3.1.1. Scanning electron microscopy

SEM surface images of the PES support as well as the neat and TiO_2/hybrid membranes are shown in Figure 1. As can be seen, the PES support shows a smooth and even surface before the formation of the PA thin layer. The images of (b), (c) and (d) are related to the neat thin layer membrane (PA), the membrane composed of 0.01 wt.% TiO_2 and the membrane composed of 0.03 wt.% TiO_2, respectively. The comparison of these images clearly showed that TiO_2 nanoparticles were uniformly distributed under the PA thin layer. In the presence of UV irradiation, the pure water flux was also increased from 20.1 L/m^2.h for the neat membrane to 32.4 L/m^2.h for the membrane composed of 0.03 wt.% TiO_2 (Figure 2). The results showed that the flux was enhanced both in the presence and absence of UV irradiation by increasing TiO_2 concentration. However, increasing the flux in the absence of UV was higher than that in the presence of UV light. The reason for this difference would be due to establishing strong hydrogen bonds and much more distribution of nanoparticles which led to a further increase of the flux in the prepared membranes in the absence of UV. On the other hand, in the presence of UV irradiation, a different mechanism occurs. Irradiation of UV ray to TiO_2 nanoparticles causes a pair of electrons and holes to appear because of semi-conductor properties of the nanoparticles. Electrons and holes react through two different mechanisms. The first mechanism leads to improving the anti-fouling properties of the membranes. In this mechanism, the reaction of the photogenerated electrons with the oxygen molecules in the surrounding membrane surface results in producing the super oxide radicals. On the other hand, the photogenerated holes react with the water molecules, leading to a generation of -OH radicals. These created reagents are strong oxidants that cause the decomposing and removal of dirt especially in organic compounds [20-23]. The second mechanism increases the hydrophilicity of the surface. Regarding the second mechanism, the photogenerated electrons reduce Ti (IV) cations to Ti (III) while the holes try to oxidize O^{2-} anions. As a result, the oxygen atoms are removed from the surface and many oxygen vacancies are produced. Accordingly, the water molecules are able to occupy the created empty sites on the surface, resulting in the creation of the adsorbed -OH groups. Hence, an increase in the surface hydrophilicity occurs [24-29]. It is supposed that by increasing the concentration of TiO_2, the second mechanism is more dominant. Accordingly, the increase of surface hydrophilicity results in the enhancement of water flux.

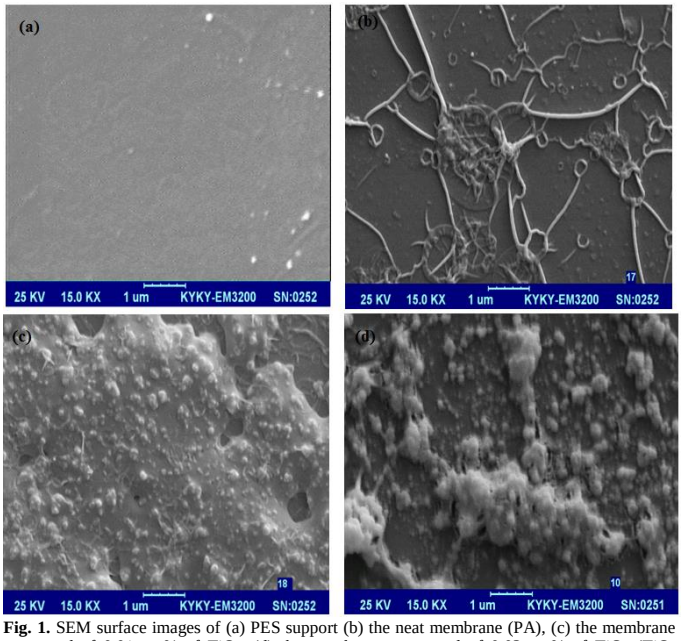

Fig. 1. SEM surface images of (a) PES support (b) the neat membrane (PA), (c) the membrane composed of 0.01 wt.% of TiO_2, (d) the membrane composed of 0.03 wt.% of TiO_2 (TiO_2 nanoparticles in aqueous phase, without UV light).

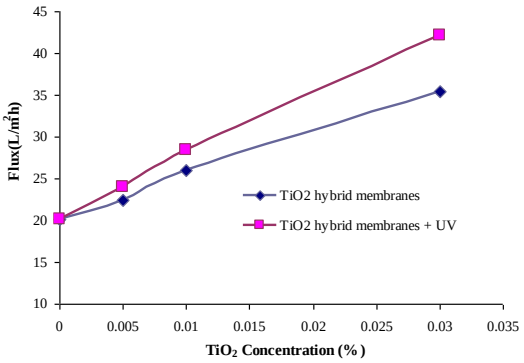

Fig. 2. Comparison of the pure water flux of TiO_2 /hybrid membranes with and without UV light.

3.1.2. Pure water flux

Figure 2 compares the pure water fluxes of TiO_2/hybrid membranes in the presence or absence of UV irradiation. As can be seen in Figure 2, the pure water flux was increased from 20.1 L/m^2.h for the neat membrane to 40.6 L/m^2.h for the membrane composed of 0.03 wt.% TiO_2 without using UV. This is due to the self-assembly of TiO_2 and establishing of strong bonds (hydrogen and coordination bonds) with the membrane polymer. Actually, the increase of hydrophilicity leads to enhancement of the flux. We believe that the presence of TiO_2 in the aqueous phase before the formation of the PA thin layer led to establishing hydrogen bonding between the surface hydroxyl group of TiO_2 and N-H groups of the PIP. The establishment of this hydrogen bonding and coordination interaction between the Ti atoms and nitrogen atoms of PIP (Figure 3) caused the TiO_2 nanoparticles to be trapped and distributed successfully under the PA thin layer. The charge was probably spread and distributed between polymer chains due to the appropriate diffusing and spreading of nanoparticles, resulting in a much higher flux.

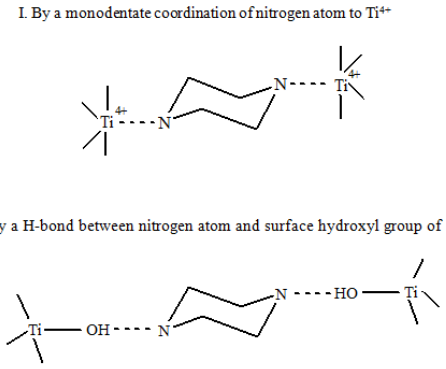

Fig. 3. Mechanism of self-assembly of TiO_2 nanoparticles under the thin-layer.

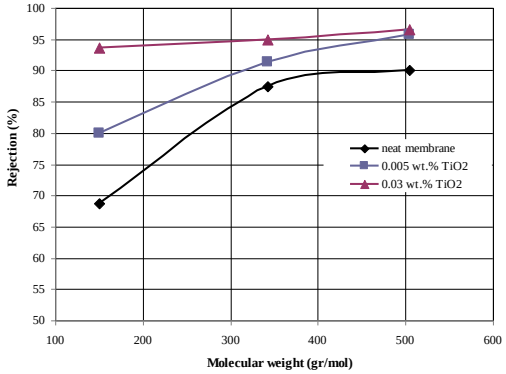

Fig. 4. Molecular weight cut-off curves of the prepared membranes without using UV (TiO_2 in aqueous phase).

3.1.3. Molecular weight cut-off

In order to prove the above statements, the molecular weight cut-off (MWCO) of the membranes was obtained by measuring the rejection capability of ribose (monosaccharide), sucrose (disaccharide) and raffinose (trisaccharide) sugars with molecular weights of 150.3, 342.3 and 504.5 gr/mol, respectively. By performing this test, the separation ability of the membranes is measured which could be attributed to MWCO. Figures 4 and 5 show the rejection capability of the obtained membranes to sugars with different molecular weights in the absence and presence of UV, respectively. As shown in Figure 4, the observed rejection of the sugars increased with the increase of TiO_2 concentration in the absence of UV. As can clearly be seen from Figure 4, the MWCO of the neat membrane and the hybrid membranes composed of 0.005 and 0.03 wt.% TiO_2 is 420, 310 and less than 150 Da, respectively. In fact, by increasing the concentration of TiO_2 the pore sizes of the prepared membranes are decreased. In short, the number of hydrogen and coordination bonds with PIP was increased and accordingly, it led to a decrease of the membrane pore sizes. On the other hand, the membrane pore sizes changed to establish and create larger pores under UV irradiation. According to Figure 5, the rejection to sugars decreased by increasing the TiO_2 concentration under UV. The sugar rejection for the membranes composed of 0.005 and 0.03 wt.% TiO_2 did not reach 90% while the MWCO of the neat membrane exposed to UV was near 410 Da. These results proved the above statements about the increase of membrane pore sizes under UV irradiation. The trapped radicals under the thin layer probably destroyed and damaged some parts of the thin film. In addition, the high energy UV irradiations could break down some hydrogen and coordination bonds with PIP along with other polymeric chain bonds, resulting in an increase in pore sizes. SEM images clearly illustrate the above claim. Figure 6 showed the SEM surface images of the membrane composed of 0.01 wt.% TiO_2 in the absence of UV (Figure 6-a) which resulted in an undamaged and integrated skin layer. On the other hand, some torn and destroyed areas over the skin layer were observed for the membrane composed of 0.01 wt.% TiO_2 under 120s UV irradiation (Figure 6-b). This process was followed and continued for the membrane composed of 0.03 wt.% TiO_2 under 120s UV irradiation. As can be seen, partial damaging of the skin layer led to the nanoparticles appearing over the surface (Figures 6-b and c). By comparing the SEM images, it clearly seems that some areas of the surface were changed and damaged under UV irradiation. Hence, increasing the pore sizes as well as the existing nanoparticles and further appearing of Ti ions on the surface leads to changing the surface charge, resulting in lower rejection for Na_2SO_4 according to the Donnan exclusion (see more detailed information in *section 3.2.1*) [30,31]. However, the membranes prepared in the presence of UV showed higher flux due to the increase of pore sizes. Anyhow, the two categories showed the pore sizes and fluxes in the range of nanofiltration membranes.

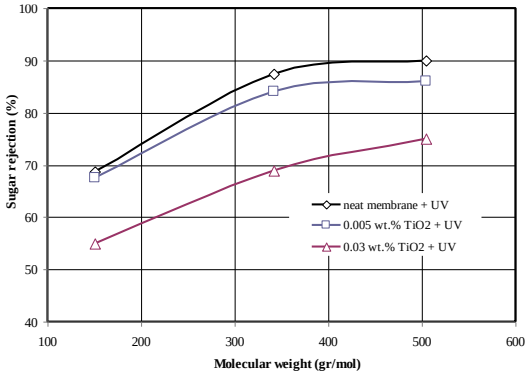

Fig. 5. Molecular weight cut-off curves of the prepared membranes using UV light (TiO_2 in aqueous phase).

3.1.4. Zeta potential

The zeta potential of the membranes was represented in Table 1. The results showed that the charge of the thin layers was changed to establish further negative charge. The neat membrane and the membrane composed of 0.005 wt.% TiO_2 showed the zeta potential amounts of about -9.7 and -11.5 mV, respectively. The increase of the negative charge was expected due to hydrogen bonds and coordination interactions. Hydrogen bonds and coordination interaction led to the space compressing of the NH groups in the PIP molecules. Accordingly, enough space for interaction of functional groups decreased which relatively led to the formation of more non-reacted functional groups in TMC molecules. Hence, the conversion of the remaining and unreacted acyl chlorides (COCl) to carboxylic acid functional groups resulted in an increase of the negative charge. Consequently, enhancing the negative charge of the membrane surfaces caused an increase in Na_2SO_4 rejection.

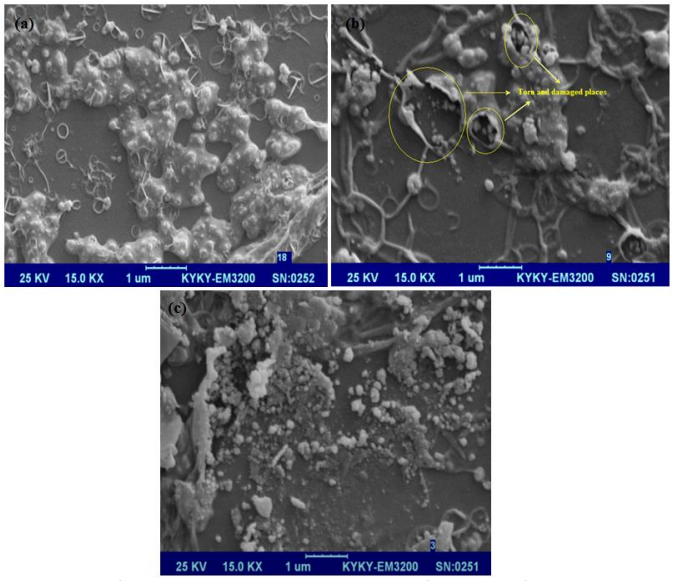

Fig. 6. SEM surface images: (a) the membrane composed of 0.01 wt.% of TiO_2 (without using UV light), (b) the membrane composed of 0.01 wt.% of TiO_2 and 120s UV irradiation, (c) the membrane composed of 0.03 wt.% of TiO_2 and 120s UV irradiation.

Table 1
Zeta potential of the obtained thin layers.

Membrane	Zeta potential (mV)
Neat Membrane	-9.7
0.005 wt.% TiO_2 in aqueous phase	-11.5
0.005 wt.% TiO_2 in organic phase	-7.4

3.1.5. Salt rejection

Figure 7 compares the rejection capability of TiO_2/hybrid membranes, with and without using UV irradiation. As can be seen, the rejection of Na_2SO_4 improved in the absence of UV from 78% to near 91%. The increase of the rejection could be attributed to both blockage and narrowing of some membrane pathways, due to the formation of hydrogen and coordination bonds, and successfully distributing and spreading the charge in the polymer structure, as previously mentioned. In contrast, the rejection of Na_2SO_4 decreased in the presence of UV irradiation from 78% to about 58%. This may be due to both increasing the membrane surface pore sizes, because of the destructive effects of UV wavelength, and changing the surface charge (see more information in *3.1.3* and *3.1.4 sections*). These results clearly show that the presence or lack of UV irradiation is a strong parameter that should be considered during membrane preparation to achieve a desirable performance and structure.

3.1.6. Fouling behavior of the prepared membranes

The flux behavior of the membranes was shown in Figures 8 and 9, respectively; during 2 h filtration of the BSA solution. The flux measurements showed that the flux of BSA solution decreased during filtration for all membranes. As can be seen, declining the flux of the neat membrane during

filtration was higher than that of the TiO_2/hybrid membranes. The results clearly revealed that the antifouling property of the TiO_2-modified membrane was significantly improved.

Table 2 represents the flux recovery ratio (FRR) data of the neat membrane and the TiO_2/hybrid membranes in the presence and absence of UV. Without using UV, the flux recovery ratio was changed and significantly enhanced from 75% in the neat membrane to about 96% in the modified membrane composed of 0.005 wt.% of TiO_2 and after that it was reduced to 87 and 85% in the membranes composed of 0.01 and 0.03 wt.% of TiO_2, respectively. Generally, the presence of TiO_2 nanoparticles has changed and improved the antifouling properties of the membranes. In fact, the increase of hydrophilicity occurred due to the presence of nanoparticles. The contact angle measurements proved that PA membranes were effectively hydrophilized via self-assembly of TiO_2 nanoparticles. As can be seen in Table 2, the contact angle values decreased from 60° in the neat membrane to 33.7° in the membrane composed of 0.03 wt. % TiO_2. However, the FRR parameter decreased at higher concentrations of TiO_2. These results may be due to the fact that in higher concentrations of TiO_2, nanoparticles showed a tendency to agglomerate because of their highly large surface area/particle size ratio, leading to reduction of the efficiency of this material. Also, lonely self-assembly of the nanoparticles on the membrane surface possesses low stability during operation [32].

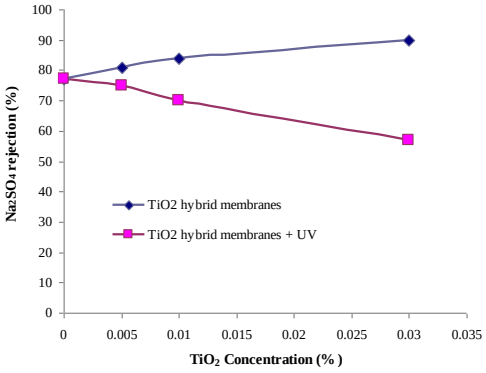

Fig. 7. Comparison of rejection of the TiO_2/hybrid membranes with and without UV light.

Table 2
Effect of different concentrations of TiO2 in aqueous phase on the membrane performance and contact angle; with and without UV light.

Membrane	FRR (%)	CA (°)
Neat Membrane	75	60
0.005 wt.% TiO_2	96	48
0.01 wt.% TiO_2	87	—
0.03 wt.% TiO_2	85	33.7
0.005 wt.% TiO_2 /120s UV	94	49.8
0.01 wt.% TiO_2 /120s UV	89	—
0.03 wt.% TiO_2 /120s UV	83	37.5

For the UV irradiated membranes, the flux recovery ratio was changed and significantly enhanced from 75% in the neat membrane to about 95% in the membrane composed of 0.005 wt.% TiO_2 and then it was reduced to 83% in the membrane composed of 0.03 wt.%. Comparing the two kinds of membranes tabulated in Table 2 approximately showed a similar trend for FRR and CA data. Actually, the anti-fouling properties of the prepared membranes were major and outstanding when lower concentrations of TiO_2 were utilized. We believe that the first mechanism occurred in the presence of UV irradiation and lower concentrations of TiO_2. As given above, the created superoxide radical anions (O^{2-}) and (-OH) radicals cause decomposing and removal of BSA molecules [33-36]. Accordingly, the antifouling properties of the membranes were increased. On the other hand, the second mechanism occurred by increasing the concentration of TiO_2, resulting in both a further increase in the surface hydrophilicity and an increase in the water flux (Figure 2). As a result, FRR enhanced from 75% in the neat membrane to 83% in the membrane composed of 0.03 wt.% TiO_2. Due to an increase in the surface hydrophilicity, a competition between adsorption of water molecules and contamination particles is observed which leads to removal of contaminations. The contact angle measurements in Table 2 were a proof for the statements above. Considering the data tabulated in Table 2, the contact angle amounts climbed down from 60° in the neat membrane to 49.8° and 37.5° in the membranes composed of 0.005 and 0.03 wt.% TiO_2, respectively. This significant decline in the water contact angle clearly indicates the creation of hydrophilicity on the membrane surface which causes changes in water flux during BSA filtration (Figures 8 and 9). On the other hand, the presence of UV prevents further formation of hydrogen bonds and coordination between PIP and TiO_2, resulting in lower dispersing and spreading of nanoparticles. Accordingly, further accumulation occurs which leads to a decrease of active sites. Consequently, as shown in Table 2, the hydrophilicity of the prepared membranes in the presence of UV was lower than that of the membranes prepared in the absence of UV. In addition, because of less formation of hydrogen and coordination bonds in the presence of UV (as stated above), the adhesion of nanoparticles to the surface is decreased which results in further removal of nanoparticles from the surface in comparison with the membranes prepared in the absence of UV.

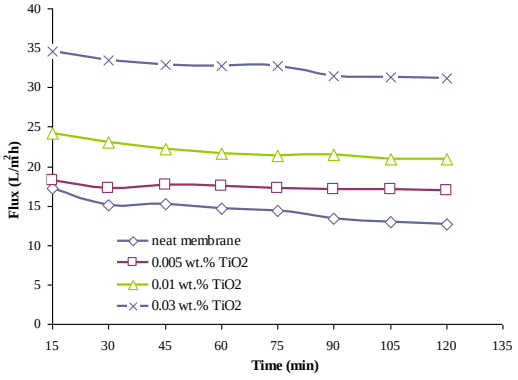

Fig. 8. Flux of the resulting membranes in the absence of UV light during BSA filtration.

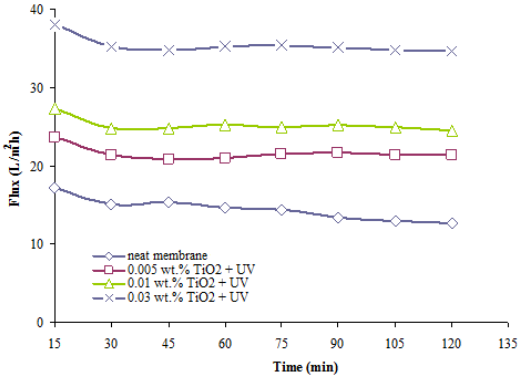

Fig. 9. Flux of prepared membranes in the presence of UV light during BSA filtration.

3.2. Effect of the presence of TiO_2 nanoparticles in the organic phase

3.2.1. In the absence of UV

Figure 10 clearly represents the pure water flux and Na_2SO_4 rejection of the prepared membranes in the absence of UV irradiation. No significant changes in pure water flux were observed while the rejection of Na_2SO_4 decreased from about 80% to near 60%. We believe that the low solubility of the nanoparticles in the organic phase caused some different behaviors.

Figure 11 shows that the rejection of sugars increased with an increase of TiO_2 concentration, but the differences were not significant and considerable. Accordingly, the MWCO of the neat membrane was 420 Da which changed to 380 and 360 Da in the hybrid membranes composed of 0.005 and 0.03 wt.% TiO_2, respectively. Hence, changing the membrane pore sizes was not

considerable.

A decline of Na_2SO_4 rejection may be due to a decrease of the negative charge of the thin layer. Zeta potential of the membranes, indicating the surface charges, was represented in Table 1. In the presence of TiO_2 in the organic phase, the negative charge of the thin layer was decreased. Two types of interactions are anticipated [11]: i) affinity of Ti atoms and carboxylic groups to create the coordination interactions and ii) formation of hydrogen bonds between hydroxyl groups of TiO_2 and carbonyl groups of polymer chains. Accordingly, a decrease of the charge is expected due to: i) abundant and huge existence of the nanoparticles over the thin layer surface and ii) coordination interaction between Ti^{4+} and the carboxylic group. Actually, the TiO_2/hybrid membranes were fabricated by self-assembly between TiO_2 nanoparticles and polymer chains including -COOH groups (Figure 12).

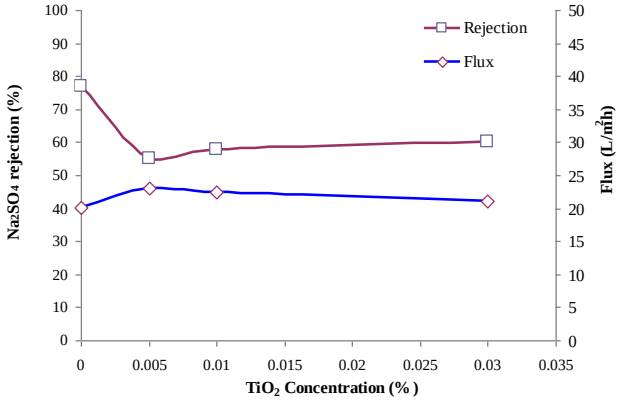

Fig. 10. Effect of TiO_2 concentration in the organic phase on the flux and rejection.

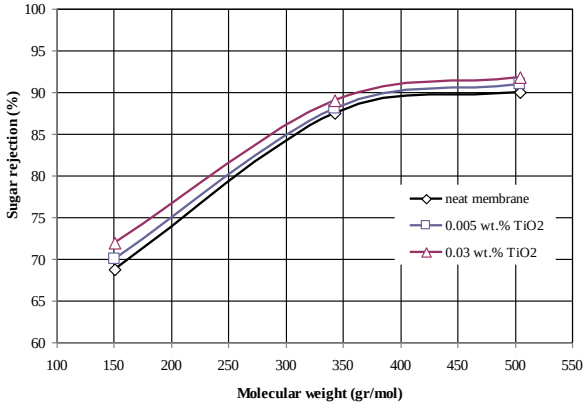

Fig. 11. Molecular weight cut-off curves of the prepared membranes without using UV (TiO_2 in organic phase).

The flux recovery ratio and contact angle measurements of the neat membrane and the TiO_2/hybrid membranes are represented in Table 3. Without using UV, the flux recovery ratio significantly enhanced from 75% to near 98% for the membrane composed of 0.005 wt.% TiO_2. On the other hand, no significant changes in FRR were observed for other hybrid membranes. The FRR of the membranes composed of 0.01 and 0.03 wt.% TiO_2 was near 97 and 96%, respectively. These results may be due to the fact that in higher concentrations of TiO_2, nanoparticles showed a tendency to accumulate and agglomerate. On the other hand, low dissolving of the nanoparticles in the organic phase caused no proper distributing and spreading of the nanoparticles on the surface. This means that a small amount of nanoparticles could diffuse into the PA thin layer body during the formation of thin layers. Accordingly, enormous amounts of the nanoparticles were established and settled over the thin layer surface. Consequently, the FRR was not changed and influenced by increasing the nanoparticles concentrations in the organic phase. Hence, high and low concentrations of nanoparticles showed a similar trend. Figure 13 shows the SEM surface images of the hybrid membranes in the absence of UV irradiation. Figures 13-a, -b and -c are related to the membranes composed of 0.005, 0.01 and 0.03 wt.% of TiO_2, respectively. These images clearly showed the huge existence and accumulation of TiO_2 nanoparticles above the surface, resulting in a high hydrophilicity of the surface. The contact angle values of the prepared membranes were shown in Table 3. As can be seen, the contact angle decreased from 60o in the neat membrane to less than 10° in the hybrid membrane composed of 0.03 wt.% TiO_2. A decline in the water contact angle refers to the increase in surface hydrophilicity.

I. By a bidendate coordination of carboxylate to Ti^{4+}.

II. By a H-bond between carbonyl group and surface hydroxyl group of TiO_2.

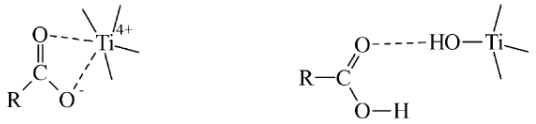

Fig. 12. Mechanism of self-assembly of TiO_2 nanoparticles on the thin-layers.

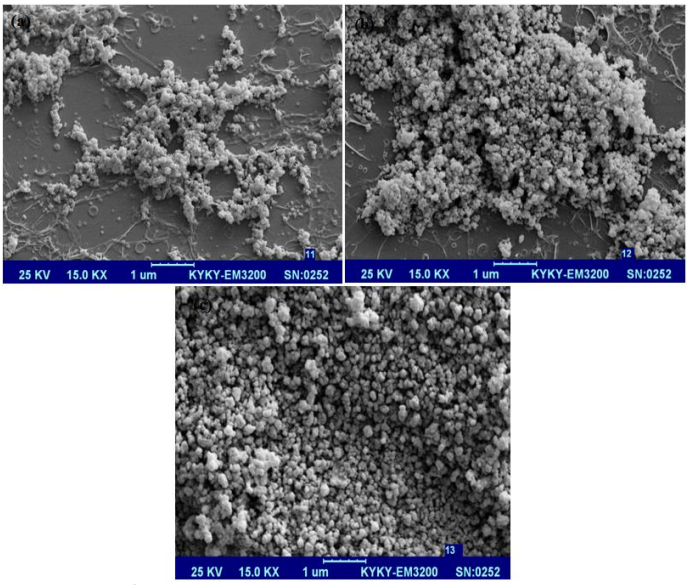

Fig. 13. SEM surface images (TiO_2 nanoparticles in organic phase, without UV light): (a) the membrane composed of 0.005 wt.% of TiO_2, (b) the membrane composed of 0.01 wt.% of TiO_2, (c) the membrane composed of 0.03 wt.% of TiO_2.

Table 2
Effect of different concentrations of TiO2 in organic phase on the membrane performance with and without UV light.

Membrane	FRR%	CA (°)
Neat Membrane	75	60
0.005 wt.% TiO_2	98	—
0.01 wt.% TiO_2	97	—
0.03 wt.% TiO_2	96	<10
0.005 wt.% TiO_2 /120s UV	97	—
0.01 wt.% TiO_2 /120s UV	87	—
0.03 wt.% TiO_2 /120s UV	85	18

3.2.2. Effect of UV irradiation

In the presence of UV irradiation, the flux enhanced due to the high hydrophilicity of the prepared hybrid membranes. On the other hand, the salt rejection indicated no significant changes (Figure 14 and Table 3). The molecular weight cut-off (MWCO) of the hybrid membranes showed no remarkable changes (Figure 15). The MWCO of the neat membrane was 410 Da which changed to 390 and 355 Da in the hybrid membranes composed of 0.005 and 0.03 wt.% TiO_2, respectively. The behavior of the prepared

membranes was similar to that of the hybrid membranes prepared in the absence of UV. The FRR amounts of these membranes decreased from 97% to nearly 85% which may be due to further destroying and breaking of the organic molecules into smaller particles, resulting in more settlement of the organic materials on the membrane surfaces and between TiO_2 nanoparticles. Another reason is less creation and production of active radicals on the surface resulting in a slight decrease of the membrane efficiency to prevent fouling phenomenon due to the accumulation of nanoparticles. As can be seen in Table 3, the contact angle values decreased from 60º in the neat membrane to 18º in the irradiated hybrid membrane composed of 0.03 wt.% TiO_2.

In summary, using UV or not, no significant differences are observed between the membranes prepared in the presence of nanoparticles in the organic phase. This may be due to not enough diffusing of nanoparticles into the PA body and structure, leading to an accumulation of nanoparticles over the surface.

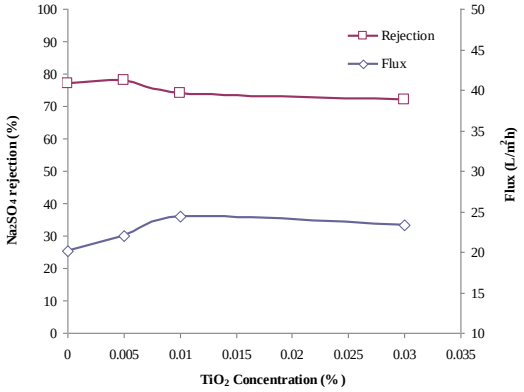

Fig. 14. Effect of TiO_2 concentration and UV irradiation on the flux and rejection.

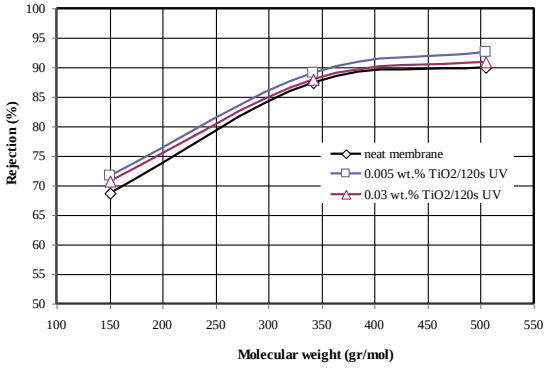

Fig. 15. Molecular weight cut-off curves of the prepared membranes in the presence of UV (TiO_2 in organic phase).

4. Conclusion

The presence or absence of UV irradiation on TiO_2 nanoparticles-assembled thin layer membranes in the aqueous and organic phases was investigated. Comparing the obtained results represented remarkable differences between the two categories of thin layers, especially on the presence or absence of UV irradiation. As a result, Na_2SO_4 rejection and the sugar separation were enhanced while using TiO_2 nanoparticles in the aqueous phase and in the absence of UV irradiation. In the absence of UV, decreasing the membrane pore sizes results in more flux recovery ratio as well as better salt rejection and sugar separation. In addition, in the aqueous phase and the presence of UV light, thin layer membranes with bigger pore sizes and higher fluxes were obtained. On the other hand, no significant differences were observed across the membranes prepared in the presence of TiO_2 nanoparticles in the organic phase.

References

[1] M.R. Teixeira, M.J. Rosa, M. Nystrom, The role of membrane charge on nanofiltration performance, J. Membr. Sci. 265 (2005) 160-166.
[2] M.R. Teixeira, M.J. Rosa, M. Nystrom, The role of membrane charge on nanofiltration performance, J. Membr. Sci. 265 (2005) 160-166.
[3] L. Lianchao, W. Baoguo, T. Huimin, C. Tianlu, X. Jiping, A novel nanofiltration membrane prepared with PAMAM and TMC by in situ interfacial polymerization on PEK-C ultrafiltration membrane, J. Membr. Sci. 269 (2006) 84-93.
[4] S. Verissimo, K.V. Peineman, J. Bordado, Influence of the diamine structure on the nanofiltration performance, surface morphology and surface charge of the composite polyamide membranes, J. Membr. Sci. 279 (2006) 266-275.
[5] P.W. Morgan, Condensation Polymers: By Interfacial and Solution Methods, Interscience, New York, 1965, pp. 19–64.
[6] J.E. Cadotte, R.S. King, R.J. Majerle, R.J. Petersen, Interfacial synthesis in the preparation of reverse osmosis membranes, J. Macromol. Sci. Chem. 15 (1981) 727-755.
[7] J.E. Cadotte, R.J. Petersen, R.E. Larson, E.E. Erickson, A new thin-film composite seawater reverse osmosis membrane, Desalination 32 (1980) 25-31.
[8] Y. Mansourpanah, S.S. Madaeni, A. Rahimpour, Z. Kheirollahi, M. Adeli, Changing the performance and morphology of polyethersulfone/polyimide blend nanofiltration membranes using trimethylamine, Desalination 256 (2010) 101-107.
[9] R.J. Petersen, Composite reverse osmosis and nanofiltration membranes, J. Membr. Sci. 83 (1993) 81-150.
[10] T. C. Merkel, B. D. Freeman, R. J. Spontak, Z. He, I. Pinnau, P. Meakin, A.J. Hill, Ultrapermeable, reverse-selective nanocomposite membranes, Science 296 (2002) 519-522.
[11] S.H. Kim, S.Y. Kwak, B.H. Sohn, T.H. Park, Design of TiO2 nanoparticle self-assembled aromatic polyamide thin-film-composite (TFC) membrane as an approach to solve biofouling problem, J. Membr. Sci. 211 (2003) 157–165.
[12] H. Yamashita, H. Nakao, M. Takeuchi, Y. Nakatani, M. Anpo, Coating of TiO2 photocatalysts on super-hydrophobic porous Teflon membrane by an ion assisted deposition method and their self-cleaning performance, Nucl. Instrum. Methods Phys. Res. B 206 (2003) 898–901.
[13] H.S. Lee, H.J. Kim, J.P. Kim, S.J. IM, B.R. Min, Preparation and characterization of TiO2–NF composite membrane and photodegradation under UV irradiation, 2, International congress on membranes and membrane processes (ICOM), Seoul, Korea, 2005, pp. 1513–1514.
[14] S.H. Son, J. Jegal, K.H. Lee, Preparation and characterization of composite NF membranes containing TiO_2 particles on their surfaces, 1, International congress on membranes and membrane processes (ICOM), Seoul, Korea, 2005, pp. 263–264.
[15] B. Rajaeian, A. Rahimpour, M. O. Tade, Sh. Liu, Fabrication and characterization of polyamide thin film nanocomposite (TFN) nanofiltration membrane impregnated with TiO2 nanoparticles, Desalination 313 (2013) 176-188.
[16] R. X. Zhang, L. Braeken, P. Luis, X. L. Wang, B. V. Bruggen, Novel binding procedure of TiO2 nanoparticles to thin film composite membranes via self-polymerized polydopamine, J. Membr. Sci. 437 (2013) 179-188.
[17] Y. Mansourpanah, E. Momeni Habili, Preparation and modification of thin film PA membranes with high antifouling properties using acrylic acid and UV-irradiation, J. Memb. Sci. 430 (2013) 158-166.
[18] Y.H. See Toh, X.X. Loh, K. Li, A. Bismarck, A.G. Livingston, In search of a standard method for the characterization of organic solvent nanofiltration membranes, J. Memb. Sci. 291 (2007) 120–125.
[19] A. Wahab Mohammad, Nora'aini Ali, Understanding the steric and charge contributions in NF membranes using increasing MWCO polyamide membranes, Desalination 147 (2002) 205-212.
[20] S.S. Madaeni, N. Ghaemi, A. Alizadeh, M. Joshaghani, Influence of photo-induced superhydrophilicity of titanium dioxide nanoparticles on the anti-fouling performance of ultrafiltration membranes, Appl. Surf. Sci. 257 (2011) 6175– 6180.
[21] N. Hilal, O.O. Ogunbiyi, N.J. Miles, R. Nigmatullin, Methods employed for control of fouling in MF and UF membranes: a comprehensive review, Sep. Sci. Technol. 40 (2005) 1957–2005.
[22] F. Liu, Y.-Y. Xu, B.-K. Zhu, F. Zhang, L.-P. Zhu, Preparation of hydrophilic and fouling resistant poly(vinylidene fluoride) hollow fiber membranes, J. Membr. Sci. 345 (2009) 331–339.
[23] N.A.Ochoa, M. Masuelli, J. Marchese, Effect of hydrophilicity on fouling of an emulsified oil wastewater with PVDF/PMMA membranes, J. Membr. Sci. 226 (2003) 203–211.
[24] O. Garp, C.L. Huisman, A. Reller, Photoinduced reactivity of titanium dioxide, Prog. Solid State Chem. 32 (2004) 33–177.
[25] M. Langlet, S. Permpoona, D. Riassetto, G. Berthome, E. Pernot, J.C. Joud, Photocatalytic activity and photo-induced superhydrophilicity of sol–gel derived TiO2 films, J. Photochem. Photobiol. A. 181 (2006) 203–214.

[26] A. Fujishima, T.N. Rao, D.A. Tryk, TiO2 photocatalysts and diamond electrodes, Electrochim. Acta 45 (2000) 4683–4690.

[27] A. Fujishima, X. Zhang, Titanium dioxide photocatalysis: present situation and future approaches, C. R. Chimie. 9 (2006) 750–760.

[28] K. Wang, J. Zhang, L. Lou, S. Yang, Y. Chen, UV or visible light induced photodegradation of AO7 on TiO2 particles: the influence of inorganic anions, J. Photochem. Photobiol. A 165 (2004) 201–207.

[29] A. Mills, N. Elliott, I.P. Parkin, S.A. O'Neill, R.J. Clark, Novel TiO2 CVD films for semiconductor photocatalysis, J. Photochem. Photobiol. A 151 (2002) 171–179.

[30] Y. Mansourpanah, S.S. Madaeni, A. Rahimpour, Fabrication and development of interfacial polymerized thin-film composite nanofiltration membrane using different surfactants in organic phase; study of morphology and performance, J. Membr. Sci. 343 (2009) 219-228.

[31] M.Y. Jeon, S.H. Yoo, C.K. Kim, Performance of negatively charged nanofiltration membranes prepared from mixtures of various dimethacrylates and methacrylic acid, J. Membr. Sci. 313 (2008) 242-249.

[32] S.S. Madaeni, S. Zinadini, V. Vatanpour, A new approach to improve antifouling property of PVDF membrane using in situ polymerization of PAA functionalized TiO2 nanoparticles, J. Membr. Sci. 380 (2011) 155 – 162.

[33] K.T. Meilert, D. Laub, J. Kiwi, Photocatalytic self-cleaning of modified cotton textiles by TiO2 clusters attached by chemical spacers, J. Mol. Catal. A: Chem. 237 (2005) 101–108.

[34] N.P. Mellott, C. Durucan, C.G. Pantano, M. Guglielmi, Commercial and laboratory prepared titanium dioxide thin films for self-cleaning glasses: photocatalytic performance and chemical durability, Thin Solid Films 502 (2006) 112–120.

[35] T. Yuranova, D. Laub, J. Kiwi, Synthesis activity and characterization of textiles showing self-cleaning activity under daylight irradiation, Catal. Today 122 (2007) 109–117.

[36] S.S. Madaeni, N. Ghaemi, Characterization of self-cleaning RO membranes coated with TiO2 particles under UV irradiation, J. Membr. Sci. 303 (2007) 221–233.